Materials Research. 2025; 28(suppl. 1): e20250121
DOI: https://doi.org/10.1590/1980-5373-MR-2025-0121

Synthesis and Characterization of Nanostructured Molybdenum Carbide through Low Temperature Gas-Solid Reaction

N. M. Santos[a]*, *M. J. S. Lima*[a], *F. E. S. Silva*[a], *C. H. R. De Paula*[a], *A. S. Silva*[a], *P. S. P. Santana*[b], *U. U. Gomes*[a]

[a]*Universidade Federal do Rio Grande do Norte, Programa de Pós-graduação em Ciência e Engenharia de Materiais, Av. Senador Salgado Filho, 3000, Lagoa Nova, 59064-720, Natal, RN, Brasil.*
[b]*Universidade Federal do Rio Grande do Norte, Programa de Pós-graduação em Engenharia Mecânica, Av. Senador Salgado Filho, 3000, Lagoa Nova, 59064-720, Natal, RN, Brasil.*

Received: January 28, 2025; Revised: August 11, 2025; Accepted: August 28, 2025

This work used ammonium heptamolybdate as a precursor to obtain molybdenum carbide (Mo_2C) at temperatures of 600°C, 650°C and 700°C, using isotherms of 60 min, 90 min and 120 min. The samples were characterized by thermogravimetric (TG), X-ray diffraction (XRD), Rietveld refinement and scanning electron microscopy (SEM). The results revealed that Mo_2C formation was strongly dependent on the source temperature and isotherm duration. Characteristic diffraction peaks of molybdenum carbide were identified in samples synthesized at 700 °C for 60 minutes and 120 minutes, indicating that this temperature was crucial for demonstrating complete carburization under the tested conditions. Conversely, samples processed at lower temperatures showed incomplete reactions, with precursor phases and residual byproducts, indicating the need for greater energy transport and reaction time to promote complete transformation into pure Mo_2C. These results reinforce the importance of simultaneously optimizing temperature and isotherm parameters to tailor the phase purity and microstructural properties of molybdenum carbide for advanced applications.

Keywords: *Molybdenum carbide, carbo-reduction, fixed bed reactor, gas-solid reaction.*

1. Introduction

Molybdenum carbide (Mo_2C) is a material of great scientific and technological relevance, widely recognized for its properties, which include high hardness, excellent electrical conductivity, corrosion resistance, and considerable catalytic activity, especially in hydrogenation and dehydrogenation processes[1-6].

In recent years, the industrial sector has shown interest in nanostructured Mo_2C materials, which exhibit properties that significantly surpass those of conventional materials. However, large-scale production still faces challenges, which has driven the search for alternative synthetic methods that are more efficient and economically viable[7-11].

Among the various factors affecting Mo_2C synthesis, temperature stands out as a crucial element, significantly influencing the structural, morphological, and functional properties of the material[11-14]. In this context, the gas–solid reaction emerges as a promising alternative, particularly for enabling carbide production at lower temperatures. The efficiency of this process is related to the close contact between the carbon molecules of the reactive gas and the solid particles of the precursor. Furthermore, the use of fine-particle precursors contributes to the advancement of the process by creating shorter diffusion paths for carbon within the solid and increasing the surface area available for adsorption. This, in turn, allows for a reduction in both the temperature and the time required for carburization[15-17].

Lira (2019) produced Mo_2C via the gas–solid reaction, using molybdenum oxide extracted from molybdenite in an H_2 and CH_4 atmosphere at a temperature of 800 °C. The resulting material exhibited a needle-like morphology, with small crystals attached to the surface, and an average crystallite size of 17.57 nm[18].

Transition-metal carbides, such as molybdenum carbide, have drawn special attention due to their importance in various industrial sectors, including special dies, aerospace, defense, and metallurgy. They also exhibit good biocompatibility, high stability, tunable band gaps, rich valence states, and excellent catalytic activity[19].

The present study aims to produce and characterize nanostructured molybdenum carbide (Mo_2C) via the gas–solid reaction, employing temperatures of 600 °C, 650 °C, and 700 °C, combined with isothermal holding times of 60, 90, and 120 minutes. The objective is to verify Mo_2C formation based on the analysis of the microstructural properties of the powders.

2. Materials and Methods

2.1. Materials

The initial powder used is: Ammonium heptamolybdate ($(NH_4)6Mo_7O_{24}.4H_2O$). The gases used for the synthesis

*e-mail: natane.martiniano.018@ufrn.edu.br
Associate Editor: Hamilton Abreu.
Editor-in-Chief: Luiz Antonio Pessan.

reactions are: Methane gas (CH_4 - 99.9% - LINE), argon (Ar - 99.9% -LINE) and hydrogen (H_2) - 99.9% - White Martins).

2.2. Methods

The samples were subjected to carboreduction to obtain Mo_2C. Table 1 shows the processing conditions.

Initially, the ground heptamolybdate powder was synthesized in a resistive tube furnace under a CH4/H2 (5/95) atmosphere. A heating rate of 10°C/min was applied until the desired temperature was reached, followed by cooling in a CH4/H2 (5/95) flow until 100°C. Argon (10 L/h) was used for cooling until room temperature.

The precursor powder was characterized by thermogravimetry (TGA) and differential thermal analysis model DTG-60H Shimadzu, X-ray diffraction (XRD) model Shimadzu XRD7000 and high-resolution scanning electron microscopy (SEM-FEG) model TM 300 HITACHI. For the samples after carboreduction, the characterizations were XRD and SEM-FEG.

3. Results and Discussion

3.1. Characterization of precursors

The XRD , the TGA/DTA and the SEM of the Ammonium heptamolybdate (HMA) was shown in Figure 1.

As shown in Figure 1(a), was possible to identify the crystalline phases according to the charts ICSD:4152 in a triclinic arrangement and ICSD:408750 in a monoclinic arrangement, showing that the powder is made up of a crystalline structure formed by several peaks that designate its crystalline planes. The pattern observed is in agreement with that described in the literature[20].

Three main events are observed in Figure 1(b), as confirmed by the DTA curve, where all the major peaks exhibit endothermic characteristics, consistent with the literature[21]. Water and NH3 were released between 112-135°C and 212-234°C. The decomposition of HMA started at 280°C and continued until approximately 330°C, resulting in the reduction to MoO3.

The morphology of the initial powder is shown in Figures 1(c) and (d). Agglomerates can be observed on the surface, indicating the dimensional variation of the material. Most of the particles are of polyhedral shape.

3.2. Characterization of the samples obtained after carboreduction

3.2.1. X-ray diffraction

The X-ray diffraction results shown in Figure 2. For those that confirmed molybdenum carbide peaks, specifically AM02, AM04, and AM05, refinement was performed using the Rietveld method, as shown in Figure 3.

Sample AM01, did not produce the desired phase for the formation of molybdenum carbide, but showed a molybdenum dioxide (MoO_2) phase. Its peaks were analyzed according to the ICSD chart: 023722 and its crystal structure is monoclinic. During the reduction process, the MoO_2 phase, subjected to a hydrogen atmosphere, is subsequently reduced to elemental molybdenum. This shows that the process of obtaining molybdenum carbide in this sample was evolving, but it was not possible to obtain it under the parameter conditions imposed, requiring more time and/or a higher temperature.

Table 1. Processing conditions - Temperature and isotherm dwell.

Samples	Temperature (°C)	Isothermal dwell (min)
AM01	600	60
AM02	700	60
AM03	600	120
AM04	700	120
AM05	650	90

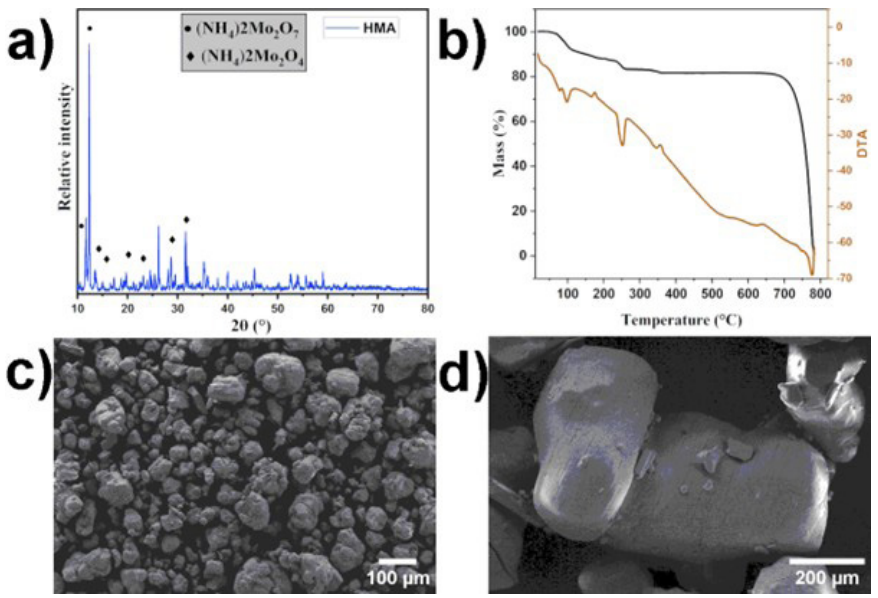

Figure 1. Initial powder characterization (a) X-ray diffraction pattern. (b) Simultaneous TGA and DTA measurements. (c) e (d) morphology.

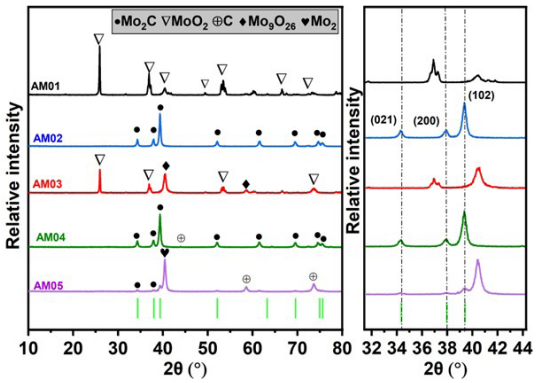

Figure 2. X-ray diffraction pattern of the samples.

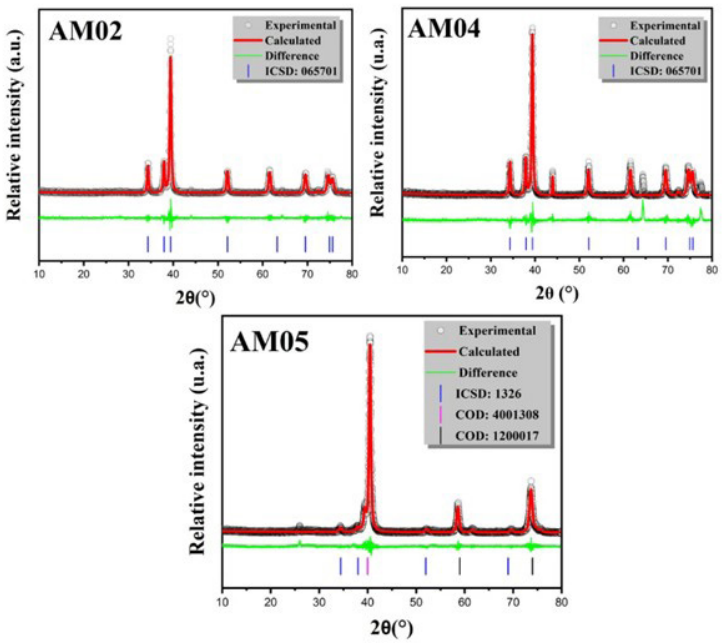

Figure 3. Rietveld refinement (experimental fit) of the samples with Mo_2C peaks.

Sample AM02 and AM04 obtained the desired phase for the formation of molybdenum carbide (Mo_2C), and were identified by the ICSD:065701 chart, with orthorhombic crystal structure. Sample AM04 has an uncharacteristic peak on the ICSD: 065701 chart, which can be seen at an angle of 44°. This peak was identified as free carbon by COD: 9012232.

Sample AM03 showed no characteristic molybdenum carbide peaks. The letter ICSD: 023722 was identified for this sample as molybdenum oxide with a monoclinic structure. Other peaks corresponding to the Mo_9O_{26} phase with a monoclinic structure were also identified for this sample (ICSD: 024031).

For AM05, the molybdenum carbide (Mo_2C) phase was identified by the ICSD:1326 chart, with an orthorhombic crystal structure. However, the peak with the highest intensity corresponds to the (211) plane, which refers to the molybdenum element (Mo_2). According to database COD: 4001308, it has a cubic crystalline structure. A C_4 peak was also identified in the diffractogram of sample (AM05), according to database COD: 1200017, and its crystalline structure is hexagonal. Figure 2 also shows an enlargement of the diffractogram patterns showing the planes of the first three Mo_2C peaks, for AM02 with the blue curve and for AM04 with the green curve.

3.2.2. Rietveld refinement

Based on the X-ray diffraction results, only the samples with molybdenum carbide phases were analyzed through refinement, as shown in Figure 3. The refinement considers an orthorhombic crystalline system for the Mo_2C phases, with a Pbcn space group. In these graphs, the ○ symbol represents the XRD profile obtained experimentally, the red line represents the profile calculated according to the data obtained in the Maud program and the green line represents the residuals, the difference between the two results mentioned.

It is possible to notice a good correlation between the experimental and calculated diffractograms, with minimal variation in the residual line. To identify whether the refinement value is close to the true value, certain indices are observed at the end of each refinement cycle. are known as quality indicators. Table 2 shows the most commonly used indices. Rwp - residual weighted profile factor, Rexp - expected factor and Sig - "Goodness of fit". The Sig index is the expected value for a good fit (sig 1), indicating a good fit between the data and the XRD patterns. This parameter relates both the structural and profile parameters and is determined for each sample analyzed. It is the ratio of the last indices. For the samples studied, the coefficient values are in line with expectations, thus indicating a good adjustment of the refinement.

After the carboreduction reaction, sample AM02 yielded the pure Mo2C phase. Sample AM04 exhibited two phases: the molybdenum carbide phase and a small percentage of free carbon. The Sample AM05 presented three phases: molybdenum carbide (16.66%), carbon (10.87%), and molybdenum (72.47%).

The average crystallite size of the samples grew as the temperature was raised, following this sequence, AM05 < AM02 < AM04. The increase in temperature causes greater electrostatic attraction and thermal agitation, favoring an increase in diameter, i.e. an increase in activation energy, favoring greater crystallinity and consequently the formation of larger particles[22,23].

3.2.3. High-resolution scanning electron microscope (SEM-FEG)

Figure 4 shows the morphology of the five samples. Figure 4(a) AM01 shows fine platelets, an indication of the molybdenum oxide phase. The presence of small, undefined particles is also noticeable; these are indicative of the presence of the molybdenum carbide phase, according to the literature[17,24]. However, X-ray diffraction analysis did not reveal any peaks characteristic of the Mo2C phase. Sample AM02 Figure 4(b) did not exhibit fine platelets, likely due to the high temperature to which it was subjected, which facilitated the conversion of molybdenum oxide to carbide.

Table 2. Refinement coefficients, crystallite size and phases present.

Coefficients	AM02	AM04	AM05
Rwp	24.76	27.77	24.44
Rexp	20.49	16.21	20.27
Sig	1.2	1.7	1.2
Crystallite size (nm)	19.7	20.5	16.94
Phase Mo2C	100%	99.52%	16.66%
Phase C	-	0.48%	10.87%
Phase Mo_2	-	-	72.47%

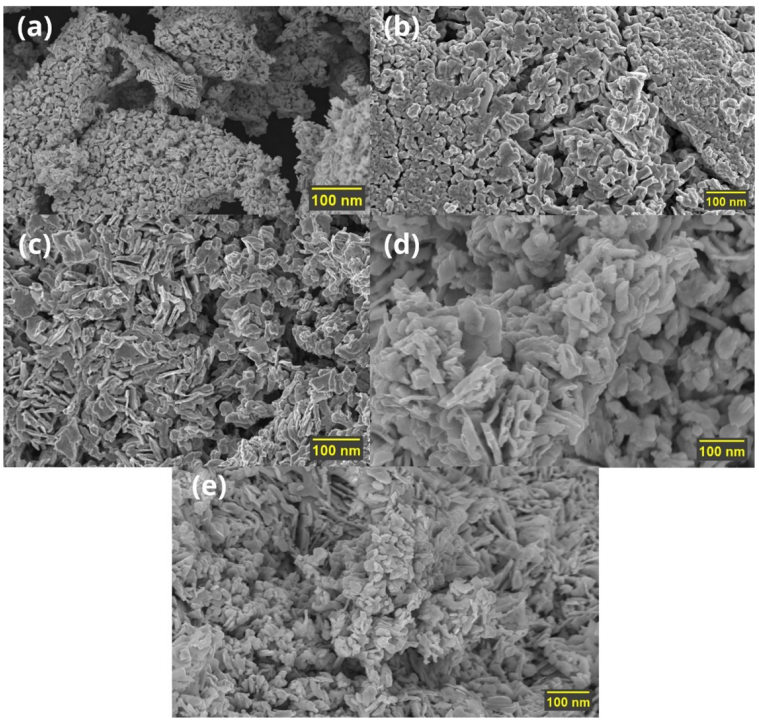

Figure 4. SEM of the samples: (a) AM01; (b) AM02; (c) AM03; (d) AM04 and (e) AM05.

For sample AM03 Figure 4 (c), the same morphology was observed, with undefined agglomerates; however, the molybdenum carbide phase was not identified by XRD, with only the MoO_2 and Mo_9O_{26} phases being detected[24].

Figure 4(d) shows the morphology observed for the carborreducing product of sample AM04. The morphology consists of undefined shapes. Therefore, the observed morphologies are similar to those of the other samples that presented the molybdenum carbide phase.

Figure 4(e) represent the morphology of sample AM05, which present undefined agglomerates, characteristic of the molybdenum carbide phase, as well as coarser needle-like shapes, characteristic of the molybdenum phase.

4. Conclusion

The molybdenum carbide production process was demonstrated efficiently, confirming the predictions of the description route employed. According to the results obtained through XRD and SEM analyses, it was possible to identify the presence of peaks characteristic of Mo_2C in samples AM02 and AM04, demonstrating the formation of the desired phase under certain description conditions. The other samples, although showing signs of carburization, did not exhibit the formation of pure molybdenum carbide, but rather secondary phases, possibly resulting in suboptimal temperature and time parameters for complete precursor conversion.

Morphological analysis revealed that the powders containing pure Mo_2C exhibited undefined cluster morphology, consistent with the literature for this type of material, confirming the influence of the gas-solid pathway and experimental conditions on the final structure. Furthermore, crystallites with sizes ranging from 16.94 to 20.5 nm were obtained, indicating the effectiveness of the approach in promoting the formation of nanostructures, a relevant aspect for catalytic and high-performance applications.

Overall, the results reinforce that precise control of temperature and isothermal time is crucial for obtaining high-purity Mo_2C with suitable microstructural characteristics. The use of relatively low temperatures, combined with the gas-solid reaction, proved to be a promising strategy for the synthesis of nanostructured molybdenum carbide.

5. Acknowledgments

This work was supported by the PIBIC CNPq (IC) scholarship.

6. References

1. Lee JS, Kim H, Han J, Park J, Choi M. Molybdenum carbides as effective catalysts for hydrogen-related reactions: recent progress and perspectives. Chem Soc Rev. 2019;48(12):2987-3014.
2. Shirvani S. Thermo-catalytic applications of two-dimensional metal carbides: (de)hydrogenation of liquid hydrogen carriers, CH4 dry reforming, and CO2 hydrogenation [thesis]. Vancouver: University of British Columbia; 2025.
3. Meena R, Bitter H, Zuilhof H, Li G. Toward the rational design of more efficient Mo2C catalysts for hydrodeoxygenation: mechanism and descriptor identification. ACS Catal. 2023;13(20):13446-55. http://doi.org/10.1021/acscatal.3c03728.
4. Zhou Z, Jia Y, Wang Q, Jiang Z, Xiao J, Guo L. Recent progress on molybdenum carbide-based catalysts for hydrogen evolution: a review. Sustainability. 2023;15(19):14556. http://doi.org/10.3390/su151914556.
5. Tong Y, Zhang Z, Hou Y, Yan L, Chen X, Zhang H, et al. Recent progress of molybdenum carbide based electrocatalysts for electrocatalytic hydrogen evolution reaction. Nanoscale. 2023;15(36):14717-36. http://doi.org/10.1039/D3NR02511J.
6. Duarte IF. Catalysts for ammonia synthesis: review and challenges for sustainable production. LAJER. 2024;11(2):73-80.
7. Wan C, Leonard BM. Iron-doped molybdenum carbide catalyst with high activity and stability for the hydrogen evolution reaction. Chem Mater. 2015;27(12):4281-8. http://doi.org/10.1021/acs.chemmater.5b00621.
8. Gomes P, Souza CP. Synthesis and characterization of nanostructured molybdenum carbide. In: XX Brazilian Congress of Chemical Engineering – COBEQ 2014; 2014 Oct 19-22; Florianópolis. Proceedings. São Paulo: Blucher; 2015. p. 13384-91. http://doi.org/10.5151/chemeng-cobeq2014-0370-25799-153524.
9. Dantas SLA, Gomes YF, Lopes-Moriyama AL, Correa MA, Souza CP. Molybdenum carbide doped with nanostructured nickel for application in degradation of reactive dyes. Ceramica. 2020;66(380):460-6. http://doi.org/10.1590/0366-69132020663802963.
10. Patel M, Subrahmanyam J. Synthesis of nanocrystalline molybdenum carbide (Mo2C) by solution route. Mater Res Bull. 2008;43 (8-9):2036-41. http://doi.org/10.1016/j.materresbull.2007.09.025.
11. Guan S, Liang H, Liu Y, Lin W, He D, Peng F. Production of silicon carbide reinforced molybdenum disilicide composites using high-pressure sintering. Ceram Int. 2020;46(15):23643-50. http://doi.org/10.1016/j.ceramint.2020.06.137.
12. Paul A, Venugopal S, Binner JGP, Vaidhyanathan B, Heaton ACJ, Brown PM. UHTC–carbon fibre composites: Preparation, oxyacetylene torch testing and characterisation. J Eur Ceram Soc. 2013;33(2): 423-32. http://doi.org/10.1016/j.jeurceramsoc.2012.08.018.
13. Xing H, Hu P, He C, Zhang X, Han J, Yang F, et al. Design of high-performance molybdenum alloys via doping metal oxide and carbide strengthening: A review. J Mater Sci Technol. 2023;160:161-80. http://doi.org/10.1016/j.jmst.2023.03.026.
14. Guo Y, Yu L, Lou XW. Carbide-based nanomaterials for electrocatalytic hydrogen production. J Mater Chem A Mater Energy Sustain. 2020;8(11):5403-10.
15. Cetinkaya S, Alp A, Aktas S, Yilmaz S. Synthesis of molybdenum carbide by gas–solid reaction using molybdenite in CH_4/H_2 atmosphere. Mater Chem Phys. 2017;202:235-41.
16. Higashi M, Ozaki T. Selective laser melting of pure molybdenum: evolution of defect and crystallographic texture with process parameters. Mater Des. 2020;191:108588. http://doi.org/10.1016/j.matdes.2020.108588.
17. Weimer, W. A. Carbide nitride and boride materials, synthesis and approcessing. 1st ed. London: Chapman & Hall; 1997.
18. Lira MMS. Production of molybdenum carbide from mineral found in the interior of Rio Grande do Norte [dissertation]. Natal: Universidade Federal do Rio Grande do Norte, Centro de Tecnologia; 2019.
19. Cetinkaya S, Eroglu S. Comparative kinetic and structural analyses of nanocrystalline WC powder synthesis from pre-reduced W under pure and diluted CH4 atmospheres. Int J Refract Hard Met. 2011;29(2):214-20. http://doi.org/10.1016/j.ijrmhm.2010.10.009.
20. Medeiros FFP, De Oliveira SA, De Souza CP, Da Silva AGP, Gomes UU, De Souza JF. Synthesis of tungsten carbide through gas–solid reaction at low temperatures. Mater Sci Eng A. 2001;315 (1-2):58-62. http://doi.org/10.1016/S0921-5093(01)01214-X.
21. Zhang Y, Wang Y, Guo C, Wang Y. Molybdenum carbide-based photocatalysts: synthesis, functionalization, and applications. Langmuir. 2022;38(42):12739-56. http://doi.org/10.1021/acs.langmuir.2c01887.
22. Oliveira VG. Preparation, characterization and luminescent properties of nickel-doped lithium zinc titanate [thesis]. Natal:

Universidade Federal do Rio Grande do Norte, Departamento de Engenharia Química; 2003.
23. Santos PTA, Freitas NL, Gama L, De Jesus AA, Andrade HMC, Costa ACFM. Synthesis via combustion reaction of NiAl2O4 catalysts for the water vapor shift reaction. J Manuf Mater Process. 2006;1(2).
24. Araújo CPB, Frota AVVM, Souto MVM, Barbosa CM, Silva MMS, Souza CP. Evaluation of two processing routes for the synthesis of molybdenum oxide with cobalt addition. Ceramica. 2019;66(377):21-9. http://doi.org/10.1590/0366-69132020663772755.

Data Availability

The dataset supporting the results of this study is not publicly available.